JOURNAL OF
EMERGING INVESTIGATORS

Article

Predicting Orbital Resonance of 2867 Šteins Using the Yarkovsky Effect

Will Rosenberg[1], Esteban Herrera-Vendrell[1]*, Raymond Nucuta[1]*, Karsen Wahal[1]*, Sarthak Bhardwaj[1], William Bryce Gallie[1], Paul McClernon[1]

[1] BASIS Scottsdale, Scottsdale, Arizona; * These authors contributed equally

SUMMARY

While gravitational forces have the largest impact on asteroid orbit determination, thermal forces such as the Yarkovsky and YORP effects also perturb asteroid orbits. We analyzed the impact of these thermal effects on the orbit of asteroid 2867 Šteins, an E-type asteroid measuring five kilometers in diameter. The orbit of Šteins lies within the range of a Kirkwood Gap, a region devoid of asteroids because of Jupiter's gravitational pull. Given that thermal effects can perturb asteroids of similar properties, we sought to determine whether the Yarkovsky effect would push Šteins into a Kirkwood Gap within 50,000 years. Based on Šteins' location and size, we hypothesized that the Yarkovsky effect will push Šteins into a Kirkwood gap. We computationally generated a thermal map of Šteins to approximate the Yarkovsky force and YORP torque. Analysis of the thermal map yielded an average Yarkovsky force parallel to velocity of -0.714 N and acceleration of -5.22 x 10^{-15} m/s^2. The torque parallel to the angular velocity due to the YORP effect was 4.680 N m, with an angular acceleration of 1.217 x 10^{-20} rad/s^2. We inputted the calculated Yarkovsky force into NASA's GMAT to model the resulting change to Šteins' orbit and found that the Yarkovsky force decays the semi-major axis of Šteins by 16.4 km in 242.2 years, and up to 5,365 km in 50,000 years within 95% confidence. This perturbation is unlikely to transfer Šteins into a Kirkwood Gap.

INTRODUCTION

In recent decades, scientists have increasingly focused on the motion of asteroids. Many people fear the risks of an asteroid hitting Earth, with NASA scientists warning of a potential collision in 2068 (1). While it was originally believed that asteroids were primarily affected by gravitational forces, recent research revealed that other forces due to the Yarkovsky effect play a role in an asteroid's trajectory. Discovered by Polish engineer Ivan Yarkovsky, the Yarkovsky effect is a force caused by the asymmetrical emission of electromagnetic radiation due to thermal radiation from rotating bodies in space (2). As the asteroid rotates, the Sun heats it, and the radiation absorbed by the asteroid is re-emitted in a different direction because of the delay between absorption and re-emission (2). This re-emission generates a recoil force in the opposite direction of the emission of electromagnetic radiation (2). Although the Yarkovsky effect exists in all astronomical bodies, it is typically observed most prominently in asteroids because asteroids have the highest surface area to mass ratios in regard to natural astronomical bodies (3).

Existing literature indicates that the Yarkovsky effect can perturb the orbit of an asteroid over long periods of time. However, research on the Yarkovsky effect remains small-scale; this study applied this effect to 2867 Šteins. 2867 Šteins is an E-type, non-family, inner belt asteroid that orbits the Sun with a semi-major axis of 2.3633 AU and an orbital period of 1327 days (4). We hoped to answer the question: will the Yarkovsky effect push 2867 Šteins into a Kirkwood Gap within 50,000 years? We investigated whether the Yarkovsky effect will push 2867 Šteins into a Kirkwood Gap within a 50000-year timespan through the use of computer modeling. We hypothesized that 2867 Šteins will be pushed into a Kirkwood gap because Šteins falls into the range of asteroid sizes significantly impacted by the Yarkovsky effect. Šteins is close to a Kirkwood Gap, which is a region of the asteroid belt largely devoid of asteroids. These gaps exist at 2.06 AU, 2.5 AU, 2.82 AU, 2.95 AU, and 3.27 AU from the Sun. Bodies with semi-major axes that reside within Kirkwood Gaps are in orbital resonance with Jupiter, resulting in a gravity assist from Jupiter that eventually propels the body out of the asteroid belt and potentially into the inner solar system (5). Due to 2867 Šteins' retrograde rotation, the Yarkovsky effect will cause it to spiral inwards towards the Sun. Therefore, the closest Kirkwood Gap inwards is considered. The distance from 2867 Šteins to this Kirkwood gap is 0.30 AU. In this study, we determined the effect of the Yarkovsky effect on pushing Šteins into a Kirkwood gap by simulating the asteroid's orbit. We concluded that the Yarkovsky effect does perturb the orbit of Šteins, but the asteroid does not enter a Kirkwood Gap.

RESULTS

To test whether or not 2867 Šteins entered a Kirkwood gap within 50,000 years, we generated a thermal map based on the Simple Thermal Model outlined by Rozitis and Green (6), assuming thermal properties from the Rosetta flyby. We implemented the model at six different positions along the orbit, calculating a force vector and torque vector from each thermal map. We modeled the resulting thermal map of one of the positions for 2867 Šteins (**Figure 1**).

The torque parallel to the angular velocity was represented by τ_P. Each force vector was broken into three directions: tangent to the velocity (F_T), perpendicular to the orbital plane (F_P), and perpendicular to the velocity and in the orbital plane (F_O). These three directions created a new coordinate axis that the force is defined on. The new coordinate axis accounted for the changing position in the orbit by defining the force vector relative to the velocity vector. Using this coordinate

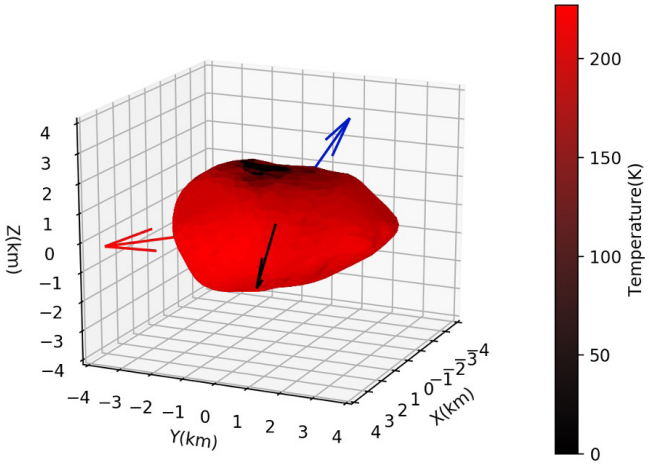

Figure 1: Thermal Map of 2867 Šteins. The thermal map of 2867 Šteins at its position on June 15, 2015 is represented. The temperature of each facet is represented through a linear color gradient. The black vector points towards the Sun, the red vector represents the direction of the velocity of the asteroid, and the blue vector displays the direction of the final Yarkovsky force vector. The off-center locations of the hottest facets shift the Yarkovsky force vector off-center against the asteroid's direction of motion.

axis, we simulated each force for one-sixth of 2867 Šteins' orbit for 242.2 years. The Yarkovsky force and torque results for each respective date were documented (**Table 1**).

The magnitude and direction of each position's tangential force relative to the other positions were plotted to visualize the calculated forces (**Figure 2**). Using the data from each position, the average tangential Yarkovsky force was calculated as -0.714 N, and the average tangential acceleration was -5.22 x 10^{-15} m/s^2. The average torque in the direction of angular momentum was 4.680 N m, and the average angular acceleration was 1.217 x 10^{-20} rad/s^2.

The results from NASA's GMAT vR2020a Orbital Determination software (7) revealed that 2867 Šteins' semi-major axis decays 16.4 km in 242.2 years (**Figure 3A**). This shift is not significant enough to push Šteins' into a Kirkwood Gap. NASA's GMAT orbital determination software (7) also revealed that 2867 Šteins' orbital inclination decays 2.35 x 10^{-9} in 242.2 years (**Figure 3B**) and 2867 Šteins' change in orbital eccentricity has a fluctuation with an amplitude greater than the average value, making the average change

Date	Position Relative to the Sun (*AU*)	Force (*N*)	τ_P (*N·m*)	F_T (*N*)	F_P (*N*)	F_O (*N*)
March 30, 2014	x = -0.530 y = 2.593 z = 0.334	x = 0.306 y = 1.236 z = 1.086	-0.056	-0.344	0.992	1.304
November 6, 2014	x = -2.226 y = 1.412 z = 0.461	x = -0.643 y = 1.060 z = 1.221	-15.027	-0.636	1.008	1.269
June 15, 2015	x = -2.290 y = -0.758 z = 0.255	x = -1.670 y = 0.200 z = 1.025	12.153	-1.050	0.753	1.487
January 22, 2016	x = -0.2421 y = -2.069 z = -0.171	x = -1.199 y = -2.217 z = -0.641	4.637	-1.063	-0.584	2.301
August 30, 2016	x = 1.959 y = -0.580 z = -0.340	x = 1.987 y = -1.583 z = -1.592	3.227	-0.812	-1.131	2.656
April 8, 2017	x = 1.520 y = 1.855 z = -0.034	x = 1.515 y = 0.797 z = 0.237	23.145	-0.377	0.371	1.646

Table 1: Yarkovsky Force and Torque vectors. The Yarkovsky force and torque vectors at each of the six simulated positions in the orbit. All position data is represented on a Heliocentric coordinate system in AU.

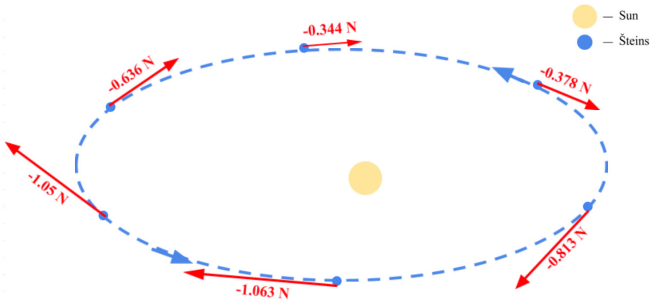

Figure 2: 2867 Šteins' Orbit Diagram. The magnitude and direction of the tangential Yarkovsky force at each simulated position in Šteins' orbit. The orbit is projected onto the XY plane and is therefore distorted to look more elliptical. Šteins is orbiting counterclockwise around the sun. The length of each arrow matches the magnitude of the tangential Yarkovsky force. This figure is not to scale.

in eccentricity over 242.2 years insignificant (**Figure 3C**).

The change in the semi-major axis, inclination, and eccentricity was forecasted for 5 time intervals with 95% confidence intervals (**Table 2**). The results from the forecasted data reveals that the maximum magnitude change in the semi-major axis over 50,000 years is 5,365 km with 95% confidence, the maximum magnitude change in the inclination over 50,000 years is -5.02 x 10^{-7}° with 95% confidence, and the maximum magnitude change in the eccentricity over 50,000 years is 6.34 x 10^{-6} with 95% confidence.

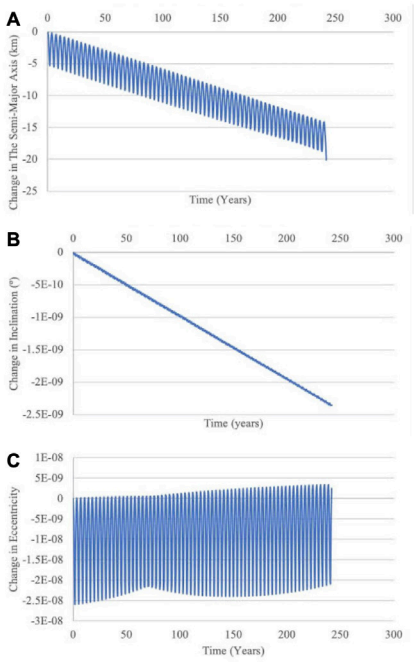

Figure 3: Orbital Elements Versus Time Graphs. Graphs of the changes in Šteins' semi-major axis, inclination, and eccentricity over the documented time period of 242.2 years during the GMAT simulation. **A)** Change in the Semi-Major Axis Vs. Time: A graph of the change in Šteins' semi-major axis (km) versus time (years) during the orbital GMAT simulation for 242.2 years. **B)** Change in the Inclination Vs. Time: A graph of the change in Šteins' inclination (°) versus time (years) during the orbital GMAT simulation for 242.2 years. **C)** Change in Eccentricity Vs. Time: A graph of the change in Šteins' eccentricity (unitless) versus time (years) during the orbital GMAT simulation for 242.2 years.

Time (years)	Change in the semi-major axis (km)	95% Confidence Radius	Change in Inclination (°)	95% Confidence Radius	Change in Eccentricity	95% Confidence Radius
250	-17.01	0.31	-2.4E-09	3.1E-12	3.3E-09	7.1E-10
500	-34.8	2.1	-4.8E-09	2.2E-11	4.6E-09	4.9E-09
1000	-59.9	6.3	-9.7E-09	6.3E-11	-7.5E-09	1.5E-08
10000	-595	214	-9.7E-08	2.0E-09	1.5E-07	5.0E-07
50000	-2950	2415	-4.8E-07	2.2E-08	7.4E-07	5.6E-06

Table 2: Orbital results of The Yarkovsky Effect. Using a forecast function and exponential smoothing, the changes in the semi-major axis, inclination, and eccentricity are forecasted over longer time spans with a 95% confidence interval documented. The three orbital elements are forecasted for five points, ending at 50,000 years.

DISCUSSION

The results indicated, with 95% confidence that 2867 Šteins will not enter a Kirkwood Gap within 50,000 years. After 50,000 years, Šteins was predicted to move 0.0065% of the 0.3033 AU necessary to enter a Kirkwood Gap. If Šteins follows the confidence interval's lower bound, Šteins will move 0.012% of the 0.3033 AU to enter a Kirkwood Gap. Thus, the minimal change in Šteins' semi-major axis provides evidence that the Yarkovsky effect does not exert a force strong enough to push e asteroids with sizes comparable to Šteins into a Kirkwood Gap. However, the Yarkovsky force does have a significant effect on the orbit of Šteins, decaying its semi-major axis by 16.4 km after 242.2 years and by up to 5,365 km in 50,000 years. This reinforced the notion that the Yarkovsky effect needs to be considered for asteroids in the sub ~20 km mean diameter range (3). However, the Yarkovsky effect can be highly dependent on the shape of the asteroid. Although the Yarkovsky effect affects the orbit of 2867 Šteins, it was not a significant force on the orbit of Šteins unless considered in the scale of orbital maneuvers. Therefore, we rejected our hypothesis that the Yarkovsky effect will push 2867 Šteins into a Kirkwood gap within 50,000 years. Future studies can analyze the seasonal effect and include more specific factors that affect the Yarkovsky force, such as the scattering and reabsorption of light. The exclusion of these factors created a source of error due to the simplification of the system to create a computer simulation, but the results from the simulation still provided insight on the magnitude and effect of the Yarkovsky effect on 2867 Šteins.

The resulting direction of the tangential force at each position matched the hypothesized direction, against the motion of the asteroid. However, the tangential force's magnitude varied between positions, with a range of 0.719 N. We hypothesized that this variation was due to variation in the asteroid's position in the z-direction, distance from the Sun, and shape. More investigation is necessary to analyze the precise causes of this variation.

METHODS

In this study, pressure from solar radiation was ignored as previous research revealed that it does not significantly alter the semi-major axis of an asteroid's orbit when considered with the Yarkovsky effect (8). Equation (1) represents the Yarkovsky force over the surface of the asteroid (9):

$$\vec{f} = -\frac{2\sigma}{3c}\oint \varepsilon T^4 \vec{n}\, ds \tag{1}$$

where c was the speed of light, σ was the Stefan-Boltzmann constant, ε was the emissivity of the surface, T was the temperature of the surface, n was the normal vector to the surface, and ds was the differential area element.

YORP, or the Yarkovsky–O'Keefe–Radzievskii–Paddack effect, is the torque that the Yarkovsky effect creates (2). When the Yarkovsky effect acts on asymmetrical bodies, it generates a net torque, causing the body to accelerate about an axis (2). This spin continuously changes the Yarkovsky force, as the rotational state (axis of rotation, period of rotation, etc.) largely determines the direction and magnitude of the Yarkovsky force (2). Equation (2) represents the YORP torque generated over the surface of the asteroid (9):

$$\vec{T} = -\frac{2\sigma}{3c}\oint \varepsilon T^4 \vec{x} \times \vec{n}\, ds \tag{2}$$

where x was the vector from the center of the body's mass to the surface. The YORP torque was not considered in the simulation of the Yarkovsky force for simplification. The results indicate that the YORP torque can reasonably be ignored because even over the time span of one gigayear, the change in angular velocity will be less than 10^{-4} percent, assuming a constant YORP torque. However, more investigation is needed to prove the insignificance of the YORP effect on 2867 Šteins.

The surface temperature of 2867 Šteins was required to quantify the Yarkovsky effect. As a result, the first step was to create a thermal map of the asteroid. The methods and equations used to compute the thermal map are modeled off of the Simple Thermal Model described by Rozitis and Green (6). The specific methods are detailed throughout the section. A stereolithography (STL) file of Šteins is made up of 1500 triangular facets, representing the surface of Šteins (**Figure 4**). The thermal map was partitioned into 50 depth-steps per facet and 400 time-steps per rotation. As Rozitis and Green demonstrate, the 50 depth-steps equally divide the depth from the surface to $2l_{2\pi}$, defined in Equation (3).

$$l_{2\pi} = \sqrt{\frac{4\pi P k}{\rho C}} \tag{3}$$

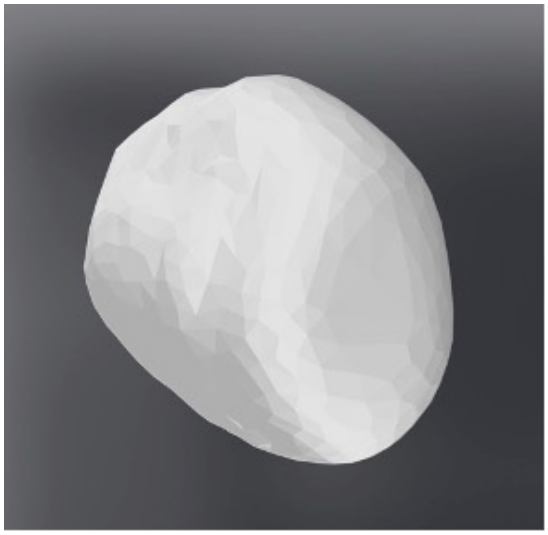

Figure 4: 3D model of 2867 Šteins. An image of the STL file of 2867 Šteins partitioned into 1500 triangular facets.

$l_{2\pi}$ was the thermal skin depth, the depth where the internal temperature lags by 2π and the amplitude of the temperature decreases by a factor of $e^{-2\pi}$ (6). The 400 time-steps equally divide P_{ROT}, or the rotation period of the asteroid.

The goal of the thermal model was to determine the temperature of each facet at any given point in the rotation. For simplicity, only 1-D heat conduction was considered, similar to Rozitis and Green (6). The thermal map was created based upon the surface boundary condition imposed by conservation of energy,

$$\left(1-A_B\right)\left(\left[S(\tau)\right]\psi(\tau)F_{SUN}\right)+\frac{\Gamma}{\sqrt{4\pi P_{ROT}}}\left(\frac{\partial T}{\partial z}\right)_{z=0}-\varepsilon\sigma T^4{}_{z=0}=0 \quad (4)$$

where A_B was the Bond albedo, $S(\tau)$ indicates whether the facet was shadowed with a 0 or a 1, Γ represents the thermal inertia, ψ(τ) returns the cosine of the Sun illumination angle, and F_{SUN} was the integrated solar flux (10) at the distance of the object, which was given by $(1367/r^2)W/m^2$ where r was the heliocentric distance of the planetary body in AU. Unlike Rozitis and Green (6), F_{SCAT} and F_{RAD} are ignored because Šteins was primarily convex, so the intensity of the light reflected and reabsorbed by the asteroid was significantly smaller than the light from the Sun. z was the unitless normalized depth variable given by

$$z=\frac{x}{\iota_{2\pi}} \quad (5)$$

and τ is the unitless normalized time variable, given by

$$\tau=\frac{t}{P_{ROT}} \quad (6)$$

Based on these relationships, the initial mean surface temperature of each facet was found using Equation (7).

$$\left\langle T_{z=0}\right\rangle_1=\left(\frac{\left(1-A_B\right)}{\varepsilon\sigma}\right)^{1/4}\frac{\int_{\tau=0}^{1}\left(\left[1-S(\tau)\right]\psi(\tau)F_{SUN}\right)^{1/4}d\tau}{\int_{\tau=0}^{1}d\tau} \quad (7)$$

S(τ) determines which facets receive light by determining whether any other facets block light from reaching it. To calculate $\psi(\tau)$, the scalar product of the vector normal to each facet and the vector representing the Sun's ray was used to find $cos(\theta)$. The solutions for $\langle T_{z=0}\rangle_1$ give the mean surface temperature of each facet over one period, which was equated to the temperatures of each respective facet and its depth steps at τ = 0. After recalculating the surface temperature at τ = 0 using Equation (4) and the value from $\langle T_{z=0}\rangle_1$, the temperature at τ = 0 was calculated at each depth step. The equation

$$T_{i,j+1}=T_{i,j}+\frac{1}{4\pi}\frac{\delta\tau}{(\delta z)^2}\left[T_{i+1,j}-2T_{i,j}+T_{i-1,j}\right] \quad (8)$$

was used where i = 1 to n depth-steps and j = 1 to m time-steps. δτ represents the length of the normalized time steps, and δz represents the length of the normalized depth steps. Equation (8) is a difference equation developed to locally approximate the differential equation for 1-D heat conduction, given by:

$$\frac{\partial T}{\partial\tau}=\frac{1}{4\pi}\frac{\partial^2 T}{\partial z^2} \quad (9)$$

The last depth step is set equal to the second-to-last depth step in order to satisfy the internal boundary condition

$$\left(\frac{\partial T}{\partial z}\right)_{z\to\infty}\to 0 \quad 10)$$

This process of iterating from the surface to the last depth-step, calculating the temperature of each depth-step for the next time-step, was repeated for at least ten full rotations and until the change in the surface temperature for the same time position was less than 0.01 to ensure that the thermal map comes to a steady state. After testing, 0.01 was chosen as the limit because it appeared the most computationally feasible, while maintaining a high level of accuracy.

The thermal map was used to calculate the Yarkovsky effect. We simulated this force within NASA's GMAT vR2020a Orbital Determination software to determine the resulting change in the orbit of Šteins (7).

We wrote all code in Python 3.6 using a class-based subsumption architecture structure. The basic structure of the code was as follows: using physical properties of 2867 Šteins, the code outputs a thermal map that generates a Yarkovsky vector that we inputted into NASA's GMAT orbital simulation software (7).

The asteroid radius, Bond albedo, density, mass, thermal conductivity, thermal inertia, position, rotation period, and spin are major factors in determining the Yarkovsky effect on 2867 Šteins. The physical parameters of Šteins are well-known and documented (**Table 3**). However, some values, such as mass and thermal conductivity, are not explicitly documented. The thermal conductivity of Šteins was estimated based on the similarity of its surface composition to enstatite (11). Given that enstatite has a thermal conductivity of approximately 4.5 W m/K (12), the thermal conductivity of Šteins was approximated as 4.5 W m/K. The mass was found by multiplying the recorded density and volume of Šteins.

A *Rays* class representing vectors of sunlight hitting the asteroid was created first. To determine which facets are shadowed, we created the class *Shadowing* with two conditions. First, all facets that faced directly away from the Sun were shadowed. We found this comparing the normal vector of each facet to the vectors of sunlight. Second, shadowing was detected in the remaining facets by determining which facets the rays intersect. This was found by calculating the signed volume of various tetrahedrons. These tetrahedrons have 5 points, including the 3 vertices of the facet and 2 random points on the ray. Once it was determined which rays intersect which facets, the code then determined which facet was intersected first using the parametric equation for the ray. If a ray of light intersected one facet before another, then the other facet that would have been hit by that ray of light was

Property	Value
Mean Radius (13)	2.7 km
Bond albedo (12)	0.24
Density (13)	1800 kg/m^3
Mass (13)	$1.368\cdot10^{14}$ kg
Thermal Conductivity (14)	4.5 W·m/K
Thermal Inertia (15)	110 J/m^2·K·s$^{1/2}$
Emissivity (15)	0.73
Position (15)	N/A
Rotation Period (15)	6.0468 hours
Spin (11)	(250.0°, −89.0°) in ecliptic coordinates

Table 3. Physical Properties of the Asteroid 2867 Šteins. The physical properties of 2867 Šteins used in the simulation of the thermal map.

"shadowed."

One addition to the shadowing class was the angle functions *phi()* and *orient()*. *phi()* returned the cosine of the angles between the normal vectors of each facet and the rays from the Sun by dividing the dot product of the normal vectors and the Sun rays by the product of the lengths of both vectors. *orient()* oriented the asteroid's north and south poles in the STL file in the direction that they are oriented in 3-D space, taking the XY-axis as the ecliptic plane. These methods were implemented in the shadowing, angle, and thermal map code. The thermal map code imported the *Rays* and *Shadowing* classes. The methods described were used to determine the temperature of each facet at different times.

Each point in an asteroid's orbit had a unique Yarkovsky and YORP vector assigned to it, based on its distance from and orientation to the Sun. To determine the Yarkovsky force vector, the thermal map of Šteins was imported, and the force due to thermal emission on the asteroid is evaluated at each time step using the approach outlined in Equation (1). The surface integral represented the net force on the asteroid at a single time step. Iterating over the entire rotation and averaging these values yielded the representative Yarkovsky force vector for that position in space. A similar approach was taken for the YORP vector, using Equation (2). The torques for all facets were taken with respect to the center of mass of the asteroid, which is given in the mass properties of the STL file. These processes were repeated for six locations to simulate the variation in the force throughout the orbit, resulting in six different vectors.

To determine the change to 2867 Šteins' orbit, NASA's GMAT software was used (7). The asteroid was simulated as a spacecraft with the Yarkovsky vector as the thrust vector. Each of the six different vectors was inputted at their respective locations. We ran the simulation for 242.2 years, using the integrator RungeKutta89 and an initial step size of 10. Microsoft Excel's FORECAST.ETS function was used on the resulting data to extrapolate the results to longer periods of time. Then, Excel's FORECAST.ETS.CONFINT was used to calculate the 95% confidence interval for the forecasted value. All astronomical measurements were taken and determined in heliocentric ecliptic cartesian coordinates.

All code for this paper can be found here: https://github.com/rnucuta/orbitalResonanceResearch.

ACKNOWLEDGEMENTS

The theory behind the Yarkovsky effect in this study was aided by the guidance of Dr. Simon Green of the Open University. We deeply appreciate the guidance of Dr. Green and the JEI editorial staff.

Received: June 12, 2020
Accepted: November 23, 2020
Published: January 26, 2021

REFERENCES

1. Whitwam, Ryan. "NASA: Asteroid Could Still Hit Earth in 2068." ExtremeTech, 28 Oct. 2020, www.extremetech.com/extreme/316690-nasa-asteroid-could-still-hit-earth-in-2068.
2. Vokrouhlicky, David, and William F. Bottke. "Yarkovsky and YORP Effects." Scholarpedia, 2012, www.scholarpedia.org/article/Yarkovsky_and_YORP_effects.
3. Bottke, William F., *et al.* "THE YARKOVSKY AND YORP EFFECTS: Implications for Asteroid Dynamics." Annual Review of Earth and Planetary Sciences, vol. 34, no. 1, 16 Jan. 2006, pp. 157–191., doi:10.1146/annurev.earth.34.031405.125154.
4. "ASTEROID (2867) Šteins." ESA Science & Technology - Asteroid (2867) Šteins, European Space Agency, 1 Sept. 2019, sci.esa.int/web/rosetta/-/43356-2867-Šteins.
5. "Kirkwood Gap: Facts, Information, History & Definition." The Nine Planets, 5 Mar. 2020, nineplanets.org/kirkwood-gap/.
6. Rozitis, B., and S. F. Green. "Directional Characteristics of Thermal-Infrared Beaming from Atmosphereless Planetary Surfaces - a New Thermophysical Model." Monthly Notices of the Royal Astronomical Society, vol. 415, no. 3, June 2011, pp. 2042–2062., doi:10.1111/j.1365-2966.2011.18718.x.
7. General Mission Analysis Tool (Version R2020a) [Computer software]. (2020, April 29). Retrieved from https://gmat.atlassian.net/wiki/spaces/GW/overview?mode=global.
8. Deo, S.n., and B.s. Kushvah. "Yarkovsky Effect and Solar Radiation Pressure on the Orbital Dynamics of the Asteroid (101955) Bennu." Astronomy and Computing, vol. 20, 2017, pp. 97–104., doi:10.1016/j.ascom.2017.07.002.
9. Pelaez, Jesus, *et al.* "A New Approach on the Long Term Dynamics of NEO's Under Yarkovsky Effect." Advances in the Astronautical Sciences , vol. 140, no. 11-440, Dec. 2011, doi: 2011AdAnS.140..440P.
10. Kopp, Greg, and Judith L. Lean. "A New, Lower Value of Total Solar Irradiance: Evidence and Climate Significance." Geophysical Research Letters, vol. 38, no. 1, 2011, doi:10.1029/2010gl045777.
11. Barucci, M. A., *et al.* "Asteroids 2867 Šteins and 21 Lutetia: Surface Composition from Far Infrared Observations with the Spitzer Space Telescope." Astronomy & Astrophysics, vol. 477, no. 2, Dec. 2007, pp. 665–670., doi:10.1051/0004-6361:20078085.
12. Sj, C. P. Opeil, *et al.* "Stony Meteorite Thermal Properties and Their Relationship with Meteorite Chemical and Physical States." Meteoritics & Planetary Science, vol. 47, no. 3, 2012, pp. 319–329., doi:10.1111/j.1945-5100.2012.01331.x.
13. Spjuth, S., *et al.* "Disk-Resolved Photometry of Asteroid (2867) Šteins." Icarus, vol. 221, no. 2, Nov. 2012, pp. 1101–1118., doi:10.1016/j.icarus.2012.06.021.
14. Leyrat, C., *et al.* "Thermal Properties of the Asteroid (2867) Šteins as Observed by VIRTIS/Rosetta." Astronomy & Astrophysics, vol. 531, 1 May 2011, doi:10.1051/0004-6361/201116529.
15. Park, Ryan, and Alan Chamberlin., "HORIZONS Web-Interface." JPL's Horizon system. 3 May 2020.